JET–P(99)04

F G Rimini et al

Combined Heating Experiments in ELM-Free H-modes in JET

JET–P(99)04

Combined Heating Experiments in ELM-free H-modes in JET

F G Rimini, P Andrew, B Balet, J Bull, N Deliyanakis,
H P L de Esch, L-G Eriksson, C Gormezano, C Gowers,
H Y Guo, G T A Huysmans, T T C Jones, R König,
M Lennholm, P J Lomas, A Maas, M Mantsinen[1], F B Marcus,
M F Nave, V Parail, D F H Start, A Taroni,
D Testa[2], P R Thomas.

JET Joint Undertaking, Abingdon, Oxfordshire, OX14 3EA,
[1]also at Helsinki University of Technology, Association EURATOM/TEKES,
02150 Espoo, Finland.
[2]also at Imperial College of Science, Technology and Medicine, London, SW7 2BZ, UK.

Preprint of a Paper to be submitted for publication in Nuclear Fusion

March 1999

ABSTRACT

High power combined NB+ICRF (H)D heating experiments have been carried out in the JET MKIIa divertor configuration, both in deuterium (DD) and in deuterium-tritium (DT) plasmas. Results from a wide range of RF injected power, up to 9.5 MW, NB power up to 22 MW, plasma currents, up to 4.2 MA, and toroidal field values, up to 3.6 T, show a clear improvement in electron temperature, DD reactivity and stored energy with respect to NB only discharges. High energy Neutral Particle Analyser (NPA) data show that acceleration of the NB injected Deuterons takes place at the second harmonic deuterium resonance. This is confirmed by numerical simulations with the PION code. Experiments have also been carried out in the (He^3)D heating scenario. ICRF heating has been an essential ingredient in the DT experiments in the ELM-free Hot-Ion regime, contributing to the achievement of a record fusion power of 16.1 MW and a record stored energy of 17 MJ.

1. INTRODUCTION

Experiments in Hot-Ion ELM-free H-modes have long been carried out at JET [1]. High confinement and DD fusion performance have been achieved transiently in this regime using Neutral Beam (NB) Heating. During the Preliminary Tritium Experiment (PTE) significant DT fusion power was first produced in an ELM-free plasma [2].

Already during the pre-PTE experimental campaign increased neutron yield was observed with combined NB and Ion Cyclotron Resonance Frequency (ICRF) heating [3]. In the MKI divertor configuration promising experiments were carried out, which showed improved confinement and performance when using ICRF to supplement NB heating in ELM-free H-modes [4], in particular in combination with Current Profile control by Lower Hybrid Current Drive (LHCD) [5,6].

The properties of ELM-free Hot-Ion H-modes with combined NB+ICRF heating have been further explored in deuterium (DD) plasmas in the MKIIa divertor campaign at high plasma current of 3 to 4.2 MA and high toroidal field of 3.4 T to 3.6 T, with total power up to 25 MW.

Despite its transient character, the Hot-Ion ELM-free H-mode has been viewed in JET as the most promising route for the Deuterium Tritium Experiments (DTE1) to achieve high DT fusion power and transient Q, thereby allowing the study of alpha particle heating [7] and Alfvén Eigenmode stability. ICRF heating has been an essential ingredient in the DT experiments in the ELM-free Hot-Ion regime, contributing to the achievement of a record fusion power of 16.1 MW and a record stored energy of 17 MJ [8].

Most of the experiments described in this paper have been carried out using ICRF tuned to fundamental hydrogen minority resonance, coinciding with the second harmonic deuterium resonance ($2\omega_{CD}$), close to the plasma center. In this (H)D scenario with ICRF only, absorption by the hydrogen minority is dominant ; the resulting fast ion tail, which is well confined for the JET

plasma parameters, extends well into the MeV energy range and provides mostly electron heating by collisional transfer to bulk electrons.

Absorption at the higher cyclotron harmonics, which strongly depends on the perpendicular velocity of the resonating particles, becomes significant in plasmas with an existing fast ion population, e.g. with NB injection, or with high bulk ion pressure [9,10]. Both these conditions are satisfied in the Hot-Ion regime, hence a significant amount of RF power is expected to be absorbed at $2\omega_{CD}$, providing direct bulk ion heating, acceleration of the injected NB ions and increased DD reactivity. Damping at $2\omega_{CD}$ has also been used in JET in the Optimised Shear Regime to achieve record DD fusion performance [11]. In TFTR core ion heating at $2\omega_{CT}$ has been demonstrated in DT supershots plasmas [12].

The extent to which the high energy tail provides bulk ion or electron heating is governed by the ratio of the typical energy of the tail to the critical energy E_{CRIT}, defined as the energy at which the collisional rate of fast particle energy transfer is the same for background electrons and ions [13]. Ion heating is privileged by minimising the resonant fast ion tail acceleration. The deuterium tail energy has been varied in the ELM-free Hot-Ion regime by splitting the ICRF power amongst up to 4 different frequencies, thereby spreading the resonance over a 30-40 cm region covering the plasma center and the low field side. Both operation with a single frequency (monochrome) and multiple frequencies (polychrome) will be discussed in the paper.

The results of experiments using different heating scenarios, (He^3)D and 2^{nd} harmonic tritium in DT plasmas, will also be presented and compared with the standard (H)D and (H)DT.

The paper is organised as follows. An overview of the combined heating experiments in ELM-free H-mode in deuterium plasmas is presented in section 2, while in section 3 the high power experiments in DT are summarised. Results of numerical simulations of both DD and DT scenarios are discussed in section 4. Finally, summary and conclusions are given in section 5.

2. COMBINED HEATING EXPERIMENTS IN ELM-FREE H-MODE IN DEUTERIUM PLASMAS

The ICRF system on JET has been designed to operate with a wide range of fundamental and multiple harmonic scenarios, with the frequency band covering the range 23 MHz to 56 MHz; each antenna consists of four independently phased straps, and there are four such antennas installed in different toroidal positions [14]. The main technical problem for ICRF heating in the ELM-free H-mode is the low coupling resistance R_C, lower, for the same plasma-antenna distance, compared with ELMy H-mode or L-mode (fig. 1). However, the absence of ELMs and large transients allows the plasma to be brought closer to the limiter, without degrading the confinement, and the antennas to be operated at high voltage. Coupling Resistance feedback control of the plasma-antenna was successfully used to maintain $R_C \cong 1.8$ -2 Ω during the ELM-free period, thereby allowing coupling of up to of 9.5 MW of ICRF power in dipole ($0\pi0\pi$) phasing at 51.2 MHz (fig. 2).

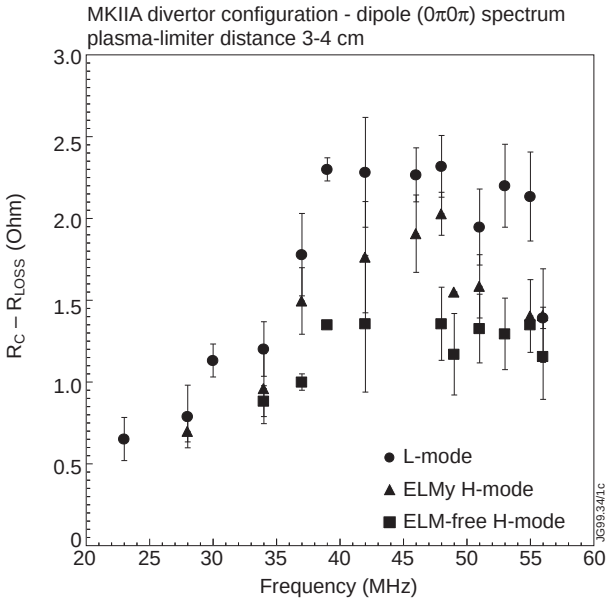

Fig.1: Coupling Resistance R_C, corrected for antenna losses R_{LOSS}, as function of frequency for MKIIa divertor discharges with plasma-Outer limiter distance 3-4 cm

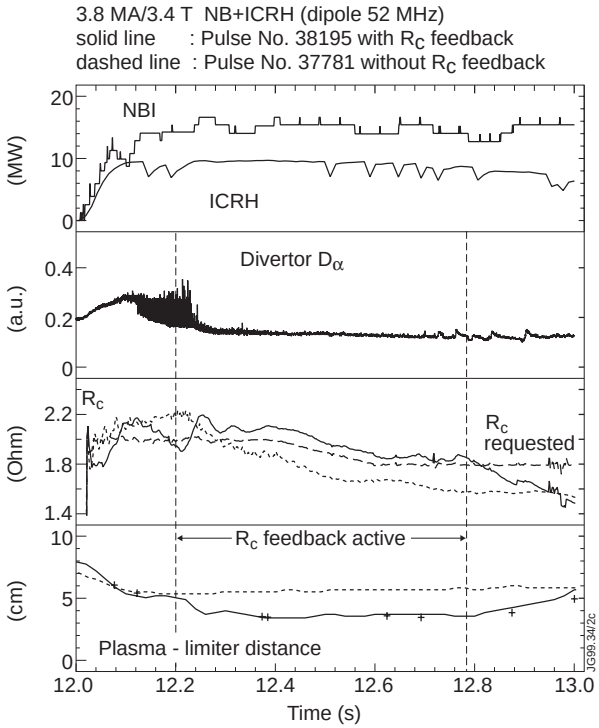

Fig.2: Operation with, Pulse No. 38195, and without R_C feedback, Pulse No. 37781 : injected NBI and ICRF power, edge D_α emission (inner divertor), requested and measured RF Coupling Resistance, distance plasma-Outer limiter

Unless otherwise specified, the experiments described in the following have been carried out in the (H)D heating scenario using multiple frequencies (polychrome) to spread the hydrogen resonance, and hence the power deposition profile, over a region extending from the plasma center to 30-40 cm on the low field side (fig. 3).

The two independent Neutral Beam D^0 injection systems are operated at 80 kV and 140 kV respectively. Real time power control [15] is used to switch off the additional heating power, in order to minimise vessel activation, once a giant ELM or a decrease in the neutron rate is detected.

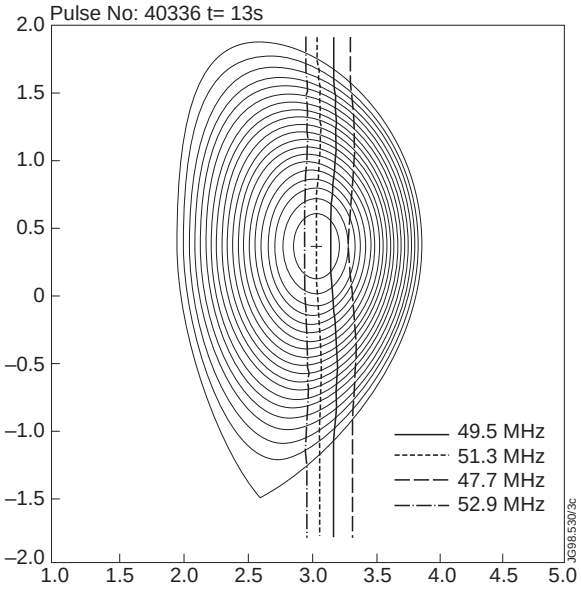

Fig.3: position of fundamental hydrogen resonance for different frequencies in a typical Hot-Ion Elm-free equilibrium at 3.45 T

In the paper the experimental data used are as follows : electron temperature from Electron Cyclotron Emission measurements, ion temperature profiles from Charge Exchange Spectroscopy, line integrated electron density measured by a Far Infrared Interferometer, and density profiles given by LIDAR Thomson Scattering.

2.1 (H)D heating scenario

The time evolution of the main plasma parameters of a NBI only and a NBI+ICRF ELM-free Hot-Ion H-mode in deuterium at 3.8 MA and 3.45 T is shown in fig. 4. Addition of ICRF to Hot-Ion H-modes results in increased core electron temperature, typically from 12 keV up to 14 keV (fig. 5). For similar power levels the electron temperature profile is more peaked with monochrome ICRF than with polychrome. An increase in core ion temperature, or the same ion temperature for higher density, is also observed. This can be attributed to a combination of two factors : firstly direct input from ICRF to the ion power balance, as will be discussed below, and secondly the effect of increased electron temperature on the ion power balance. Simulations with the TRANSP code [16] suggest that in the combined heating case ion-electron equipartition is substantially reduced, up to half of the calculated value in the NBI only case. The higher electron temperature also translates into higher values of the critical energy E_{CRIT} at which the injected beam ions heat electrons and bulk ions at equal rate, typically for these plasmas in the range of 200-250 keV, and therefore a higher fraction of ion heating with respect to electron heating.

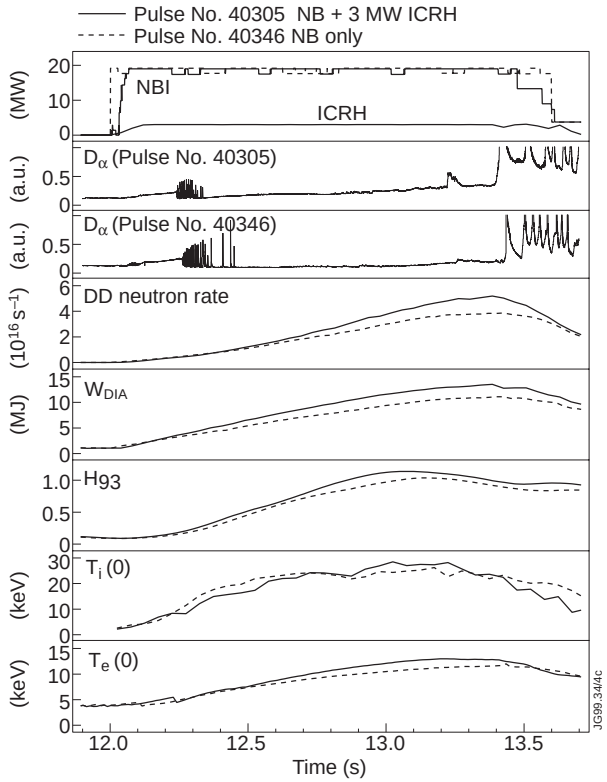

Fig.4: time evolution of main plasma parameters for Hot-Ion ELM-free H-modes with NB only (Pulse No. 40346) and NB+ICRF (Pulse No. 40305). From top : injected NB and RF power, edge D_α emission (inner divertor), DD neutron rate, diamagnetic stored energy W_{DIA} , ratio H93 of thermal confinement time to the value predicted by the ITERH93-P scaling, core ion and electron temperatures.

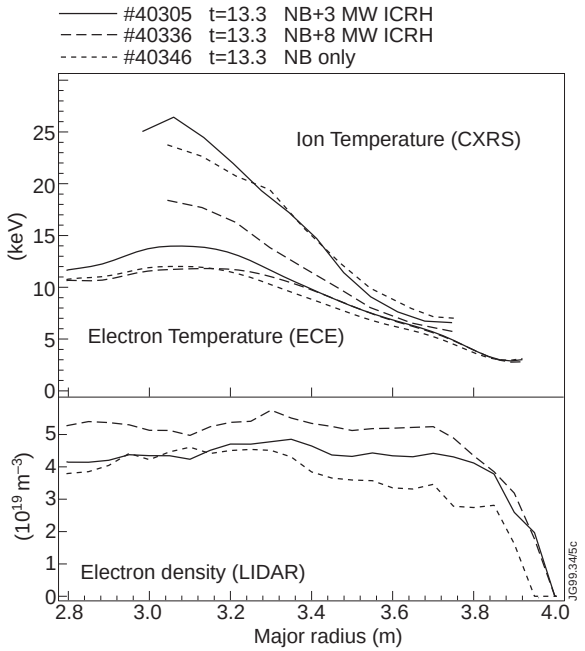

Fig.5:radial profiles of ion and electron temperature and electron density, taken close to the peak of performance but before any observable MHD activity, for NBI only and NBI+ICRF with two different levels of RF power. Note that the NBI only discharge has no gas flow.

The maximum stored energy reached at the end of the ELM-free phase is also increased by the addition of ICRF, up to a record, for the Hot-Ion H-mode in DD, of 14.5 MJ with 25 MW of total heating power. The contribution to the stored energy from NBI and ICRF driven fast ions is estimated to be up to 2 MJ at the beginning of the ELM-free phase, and < 2 MJ around the peak of neutron emission for discharges with RF power above 4 – 5 MW; for RF power below 4 MW it is in the range of 0.5 - 1 MJ. TRANSP calculations indicate that the heat diffusion coefficient χ_{eff} is similar to the NB only discharges. The total thermal confinement, normalised to the ITERH93-P ELM-free scaling [17], is higher in NB+ICRF than in NB only cases (fig. 4). This is in agreement with what has already been observed in MKI combined heating ELM-free experiments [18] and in general in discharges with peaked rather than broad power deposition profiles.

For comparable levels of total input power, discharges with ICRF show higher values of D_α and CIII light in the main chamber, with increased ratio of carbon to deuterium recycling (fig. 6). No significant differences are found in the recycling and impurity influxes in the divertor region; the higher recycling is seen even at modest RF power levels, but appears to increase with RF power.

A continuous gas bleed, which seems to be beneficial for controlling the impurity level and possibly the edge MHD activity [19], is used during the ELM-free phase of combined heating discharges. This, in combination with the already mentioned increase in recycling, results in slightly higher edge density and broader NB deposition profile than discharges with NB only or without gas input (fig. 5). With increasing ICRF power the density increase during the ELM-free phase is stronger, due to the increased main chamber recycling and impurity influx: as a consequence, the impurity level in the plasma is increased, the NB deposition profiles are broader, ion temperature is lower (fig. 5) and the heat flux through the separatrix, P_{LOSS}, increases rapidly.

Statistically, the maximum length of the high performance phase tends to decrease with increasing input power. The data suggest that NB+ICRF cases are comparable to NB cases at similar power level (fig. 7). However for a

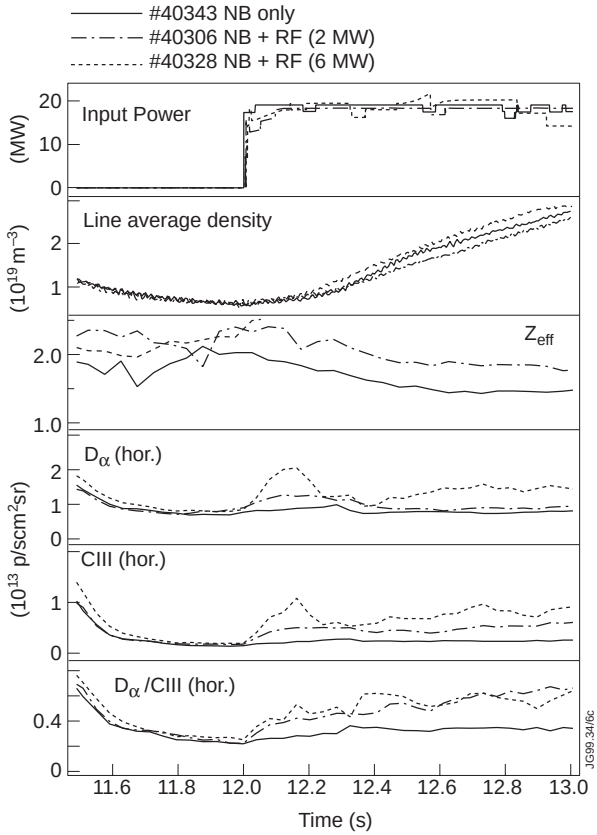

Fig.6:Hydrogenic species and light impurity recycling, for the same input power, for NB only (Pulse No. 40343) and combined NB+ICRF discharges (Pulse No. 40306 and 40328). From top : total input power, line average density and Z_{eff}, D_α and CIII photon flux for horizontal (main chamber) line of sight, and ratio of CIII to D_α flux.

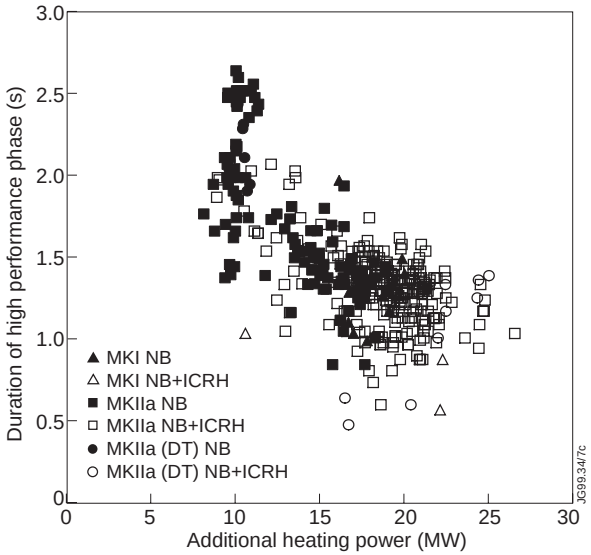

Fig.7: duration of the high performance phase, from start of high power pulse to terminating MHD event, vs. additional heating power for discharges with I_{pla} > 3.4 MA

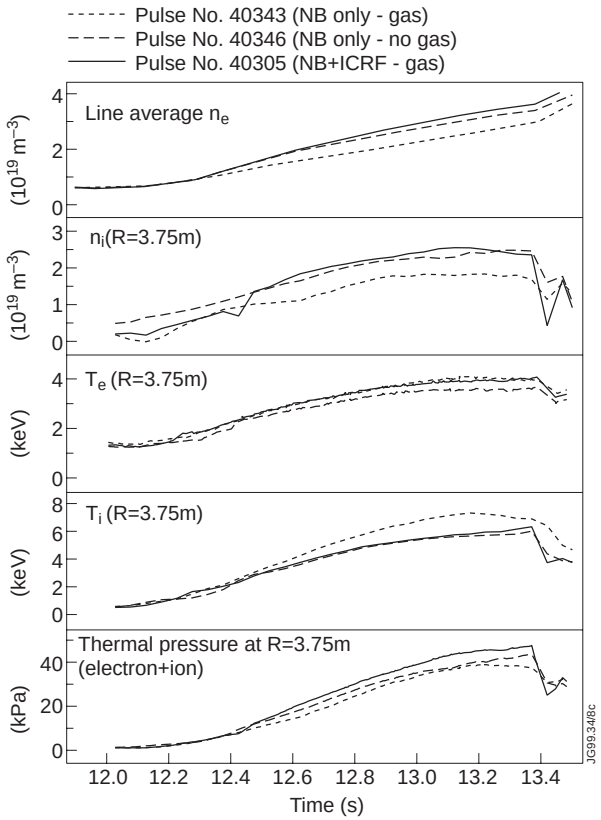

Fig.8: comparison of temperature and density evolution close to the edge transport barrier, R=3.75m, for NBI only discharges, with and without gas fuelling, and NBI+ICRF

a given total input power the typical duration of the ELM-free phase appears to be reduced when the proportion of ICRF to NBI power increases.

On the other hand, there is evidence that discharges with NB + modest ICRF (3-4 MW) reach the terminating ELM event at higher values of stored energy than with NB alone, even when the fast ion contribution to the diamagnetic stored energy W_{DIA} is taken into account. Measurements of edge density, ion and electron temperature close to the position of the edge transport barrier suggest that the maximum pedestal pressure, before the giant ELM, is higher with NB+RF than with NB alone (fig. 8). A detailed analysis is in progress, but already numerical analysis, carried out both with the TRANSP code and with a simplified model for NB [20], do not suggest significant differences in the fast ion population in the outer plasma region in the two types of discharges. ICRF is not expected to contribute directly, either because of orbit effects or because of interaction with NB injected ions, to the fast particle population in this region [21].

In the standard Hot-Ion ELM-free regime, high power is injected when sawteeth are already present; the occurrence of a large sawtooth late in the ELM-free phase leads inevitably to a performance degradation which extends beyond the q=1 surface and it is often followed closely by a giant ELM [22]. In the MKI divertor campaign it was found that Hot-Ion ELM-free H-modes with combined heating were mainly terminated by sawtooth activity, unless LHCD was

used to broaden the current profile [5,6,18]. The observation of sawtooth-free periods in Hot-Ion H-modes is not understood: equilibrium reconstruction with the EFIT code indicates that, within the error bars, q(0) remains below 1 during the ELM-free phase. On the other hand, in NB only discharges the fast ion injection energy does not seem to be sufficient for fast particle stabilisation of the unstable internal kink mode. Calculations for MKIIa high performance deuterium and DT discharges show, however, that a significant stabilising contribution can arise from ICRF driven hydrogen ions [23], and it is found experimentally that discharges with modest RF power exhibit good stability with respect to core MHD. In common with NB only pulses, the high performance phase of these discharges terminate generally with a combination of external kink modes, the so-called Outer Modes, and a giant ELM. As a result of the identification of the Outer Mode as an ideal external kink, driven by the edge current gradient [24], a method for mitigation of the Outer Mode by a continuous current ramp down at ~ 0.2 MA/s during the ELM-free phase was successfully developed, and was used in all the experiments discussed in this paper [19].

Measurements of magnetic fluctuation spectra, with up to 1 MHz sampling rate, indicate that core localised Toroidal Alfvén Eigenmodes (TAE) can be excited during the high performance phase of combined heating Hot-Ion ELM-free discharges [25]. These modes are thought to be driven by trapped energetic ions with energies above 500 keV [26], which can be easily produced by (H)D minority. An ICRF power threshold for excitation of AE modes has been identified : discharges with 3 MW of RF power in polychrome scenario do not show the presence of TAE, which can however be seen above the 4 MW power level. In such conditions, the amplitude of the AE decreases with time, until they disappear completely close to the peak of performance [27].

Discharges with NB + ICRF are characterised by increased DD neutron yield (fig. 2) up to 5.2 x 10^{16} neutrons/s, which is the highest DD yield ever achieved in the ELM-free Hot-Ion scenario. The scaling of DD neutron yield with total input power and stored energy (fig. 9) appears to be similar for NBI only and NB+ICRF discharges with modest ICRF power. With increasing ICRF power and fraction of ICRF to NBI power, the discharges tend to deviate from this scaling, moving towards high stored energy but not to higher DD reactivity. This can be linked to a combination of reduced ELM-free phase duration, broader NBI deposition profiles, increased impurity content and lower ion and electron temperatures, as discussed above. As already mentioned, these discharges also exhibit TAE activity, but it is

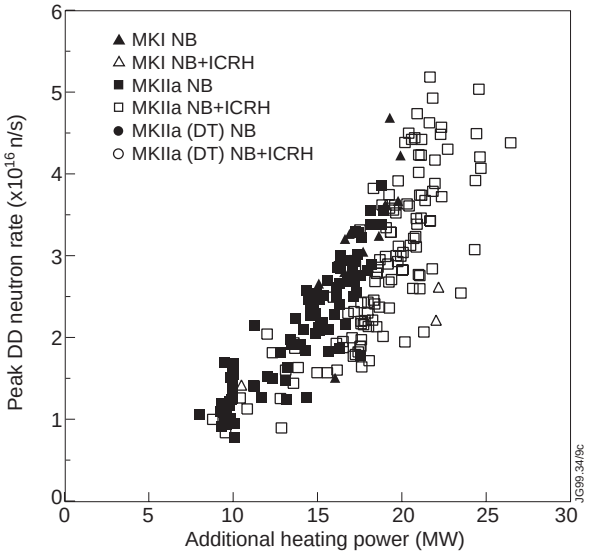

Fig.9: peak DD neutron rate vs. additional heating power for discharges with I_{pla} > 3.4 MA

not obvious if and by how much the TAE activity can contribute to the performance degradation. On the other hand, TAE activity may well broaden the fast ion profile and thereby compromise sawtooth stabilization by the fast ions, which relies on a strong fast ion population within the q=1 surface.

Data from the High Energy Neutral Particle Analyser (NPA) [28] show the presence of deuterons above the injection energy of the beam ions, 80 and 140 keV, indicating that some of the ICRF power is coupled to deuterons at the 2^{ND} harmonic resonance. This is in agreement with theoretical expectations on the competition between fundamental hydrogen resonance and the degenerate $2\omega_{CD}$ in conditions of low hydrogen concentration, typically << 5 % in these plasmas, and high deuteron pressure. In general, deuteron counts in the highest energy channels, ≥ 0.8 MeV, are barely above the noise level. Fig. 10 shows results from an experiment aimed at minimising the fraction of ICRF power absorbed at $2\omega_{CD}$ by increasing the concentration of the hydrogen minority, and therefore the fraction of power absorbed at the fundamental hydrogen resonance. The hydrogen concentration, as measured at the plasma edge by visible spectroscopy, is increased to 8 - 10 % at the end of the ELM-free period. As a result, the deuteron acceleration is much reduced and there is a clear delay in the appearance of high energy deuterons until late into the high performance phase. It has to be noted that, although the DD reaction rate is reduced, the H-mode performance in terms of ELM-free period and confinement is not affected by the increased hydrogen concentration. The measurements also indicate that the deuterium tail driven by ICRF is more evident at high RF power density, i.e. high RF power and/or monochrome operation. In the absence of strong MHD activity, the perpendicular tail temperature inferred from the line integrated NPA deuterium distribution function scales as

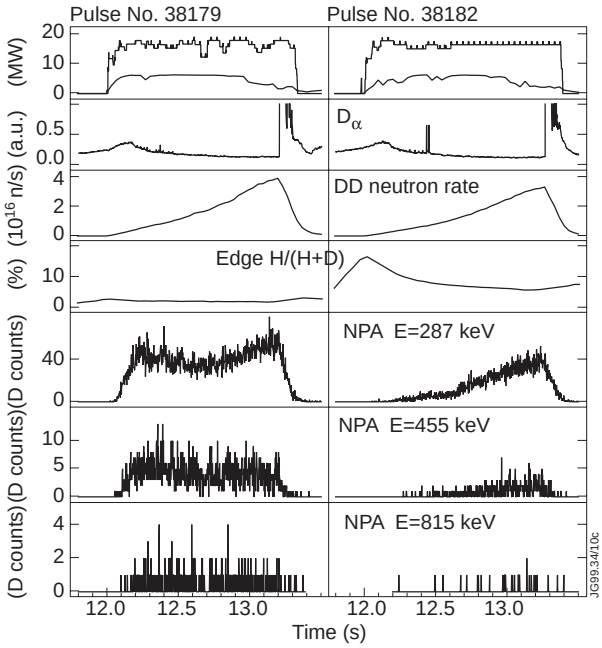

Fig.10: NPA measurements of fast deuteron population for low (Pulse No. 38179) and high hydrogen content (Pulse No. 38182). From top : input power, edge D_α, DD neutron rate, edge hydrogen concentration and deuteron counts in three different NPA energy windows.

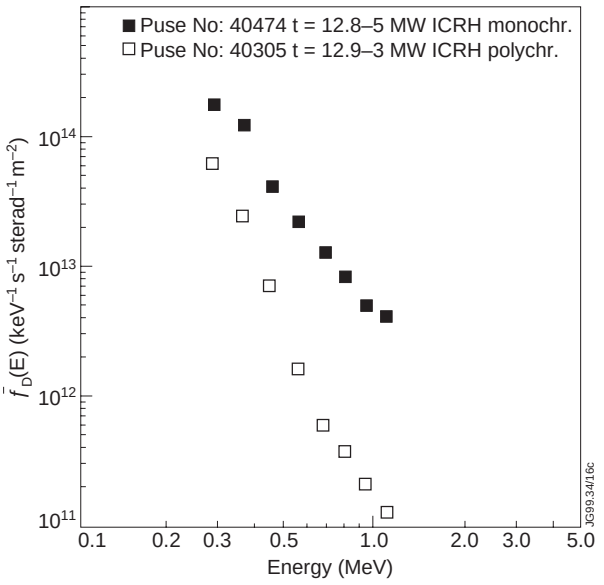

Fig.11: NPA line integrated deuteron distribution function, at pitch angle π/2, for two different ICRF heating scenarios

$T_{Tail} \propto P_{ICRF} * \tau_{SD} / n_{D,fast}$; here τ_{SD} is the deuterium slowing down time and $n_{D,fast}$ is the measured fast deuterium density. For the two cases in fig 11, despite the fact that the values of $P_{ICRF} * \tau_{SD} / n_{D,fast}$ are similar, the measured tail temperature is clearly higher in the monochrome than in the polychrome discharge. Ion heating from collisional transfer from fast to bulk deuterons should, therefore, increase when using polychrome operation at modest RF power levels.

2.2 (He^3)D heating scenario

A limited number of discharges have been carried out using the (He^3)D heating scenario at 3.8 MA/ 3.45 T, with ICRF power ranging from 2 to 5 MW. Heating at the fundamental He^3 resonance has long been explored in JET [29] and has recently been exploited in the DTE1 campaign to generate bulk ion heating in ICRF only discharges [30].

RF theory predicts that minority heating at ω_{He3} should yield more ion heating than the minority ω_H scheme, because the high mass and low mass to charge ratio of He^3 would result in less energetic minority tail and higher critical energy E_{CRIT}. Unfortunately, as it will be discussed later, the comparison with the (H)D scheme is complicated in the Hot-Ion scenario by non-negligible, ~40-50 %, damping at $2\omega_D$ which can also supply some direct and indirect ion heating. The (He^3)D heating scenario also suffers from a weak damping per pass and competition from direct electron damping could be important, especially in the high electron pressure conditions of the Hot-Ion regime.

For the experiments described here comparison of DD fusion performance with typical Hot-Ion discharges is also made difficult by the contamination of plasmas with tritium, in the range of 3 – 4 % of the density, and hence by the high level of DT neutrons, which contribute to up to 50 % of the total neutron rate.

He^3 is injected in the plasma 0.1 s before the NB+ICRF heating. The core He^3 concentration, measured by Charge Exchange Recombination Spectroscopy, has been varied from ~ 2 % up to ~ 10 %. With increasing He^3 concentration, a reduction in neutron rate due to core pollution has been observed.

A comparison of NB+ICRF discharges with similar levels of NB and RF power, #42371 with (H)D and #42404 with (He^3)D heating, is shown in fig. 12., together with the best NBI only discharge of MKIIa, #40346,

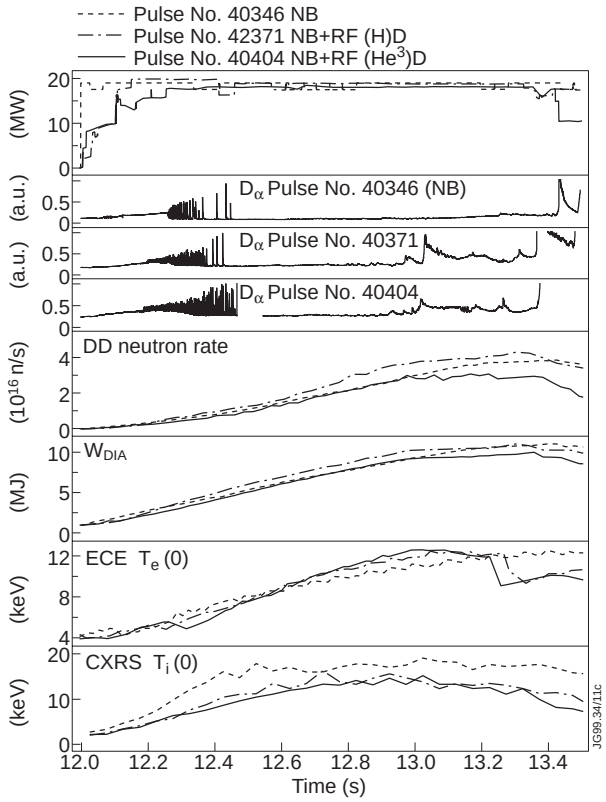

Fig.12: time evolution of plasma parameters for NB only (Pulse No. 40346), NB+ICRF-(H)D (Pulse No. 42371) and NB+ICRF-(He^3)D (Pulse No. 42404). from top : additional heating power, edge D_α, DD neutron rate, diamagnetic stored energy, central electron and ion temperatures.

which has approximately the same total input power. Discharge #42404 has 3 - 4 % He3 concentration. In the two combined heating cases electron and ion density and bulk ion temperature are similar. At the beginning of the high power pulse $T_e(0)$ increases faster in the (H)D case, and the last sawtooth happens earlier ; such differences, although within the typical variability of the ELM-free Hot-Ion regime, may be a result of the different fast ion distribution. Towards the end of the ELM-free phase the electron temperature profile appears to be more peaked in the (He^3)D case, and $T_e(0)$ is also marginally higher. The high performance phase is terminated in both cases by an Outer Mode, followed by a sawtooth and a giant ELM. The diamagnetic stored energy W_{DIA} is higher by about 1 MJ in the (H)D case, which again is suggestive of a difference in the fast ion component. The fact that the (H)D pulse has about 2 MW more of injected NB power for the first 0.4s is probably significant in the light of the general experience with ELM-free Hot-Ion H-modes, but it is difficult to quantify in terms of its effect on performance.

A rough estimate of the DD neutron rate, taken as the difference between the total and the DT neutron rate, suggests that DD reactivity is higher in the (H)D case by about 20 - 25 %. Since the bulk ion pressure is very similar in the two discharges, the excess DD neutrons can be attributed to acceleration of beam particles at $2\omega_{CD}$.

The NB case has clearly higher Ti(0) and DD reactivity and lower Te(0), but also much higher NB power during the first 0.2s. The NB+ICRF case, however, shows a continuous increase of ion temperature until the Outer Mode appears, while in the NB pulse $T_i(0)$ saturates.

3. HIGH POWER HOT-ION ELM-FREE EXPERIMENTS IN DT PLASMAS

Following the positive experience in deuterium plasmas, ICRF was used in most of the deuterium-tritium (DT) experiments in the ELM-free regime [8].

The DT Hot-Ion experiments were carried out first in the standard 3.8 MA / 3.4 T scenario and later at 4.2 MA / 3.6 T. For the first set of experiments, the same ICRF frequencies cases were used as in the DD, while at higher field the full frequency range of the ICRF antennas was exploited, using up to 57 MHz for (H)D and 37 MHz for the $2\omega_{CT}$ scenario.

In the high power discharges considered here the walls were loaded with ohmic and ICRF heated pulses until the measured plasma mix was close to 50:50 DT. A DT continuous gas bleed was also used, as in the DD discharges, although with a slightly higher flow. The standard polychromatic hydrogen minority scenario at 3MW power level was used for most of the DT experiments, but a combination of hydrogen minority and 2^{nd} harmonic tritium heating at higher RF power was also tried. For DTE1 one of the NB systems was converted to inject 100 % tritium at up to 155 kV energy, while the second NB system injected 100 % deuterium at 80 keV. The total NB power available was in excess of 22 MW, higher than in the DD campaign.

A direct comparison of NB only and NB+ICRF has been carried out at 3.8 MA / 3.4 T. The combined heating case delivered 12.9 MW of fusion power for 22.4 MW of total input power, while the NB only case reached 12.3MW of fusion power with 21.3 MW of input power. The instantaneous power gain, defined as $Q_{IN} = P_{DT} / P_{IN}$, is ~ 0.57 for both discharges. The time evolution of the main plasma parameters for both discharges is shown in fig. 13. For the combined heating discharge, as a test, about 0.5 MW of RF power tuned for central $2\omega_{CT}$ were added 0.5 seconds into the ELM-free phase.

In both cases the tritium concentration varies from 40 %, measured by the D_α and T_α intensity at the plasma edge, to 50 %, as indicated by Neutral Particle Analyser data.

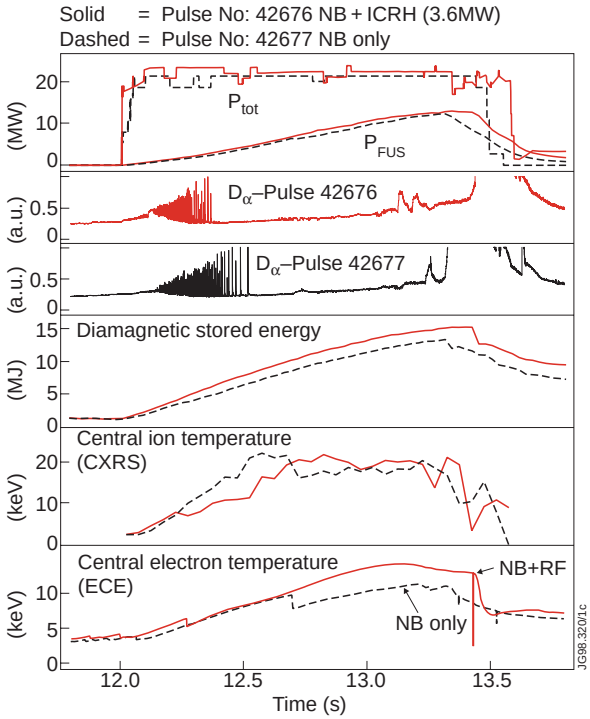

Fig.13: time evolution of plasma parameters for DT discharges at 3.8 MA / 3.4 T with NB only (Pulse No. 42677) and NB+ICRF (Pulse No. 42676). From top : additional heating and DT fusion power, edge D_α, diamagnetic stored energy, central ion and electron temperatures.

The comparison of the discharges is made difficult by the fact that the NB only discharge suffers from a large sawtooth halfway through the high performance phase The analysis of the stability of DT plasmas in the Hot-Ion ELM-free regime with respect to core and edge MHD is presented elsewhere [23], and there are indications that the fast ion population driven by ICRF strongly contributes to stabilisation of sawteeth. The central electron temperature reaches 14 keV in the NB+ICRF case, before a degradation is observed coinciding with the appearance of edge MHD activity ; in the NB case $T_e(0)$ recovers well after the sawtooth, reaching ~ 11 keV. The central ion temperature is in the range of 23 keV for the NB+ICRF case and marginally lower, ~22 keV, with NBI alone.

The diamagnetic stored energy just before the giant ELM is above 15 MJ in the combined heating pulse and around 13.5 MJ with NBI only. The corresponding thermal stored energy is in the region of 12 MJ in both cases.

A second set of NB+ICRF experiments at 4.2 MA / 3.6 T was carried out, using the full NB power available, ~ 22 MW, and taking advantage of the increased confinement and MHD stability of the high current and toroidal field. A new record DT fusion power of 16.1 MW was achieved, together with a record diamagnetic stored energy in excess of 17 MJ, with 25.4 MW

of combined additional heating and ICRF tuned to hydrogen minority. The time evolution of the plasma parameters and the MHD behaviour of these record pulses is similar to the DD and DT cases at 3.8 MA / 3.4 T.

A mixed (H)D and $2\omega_{CT}$ scenario was also tested at high current, with 3 MW on the hydrogen resonance and ~ 2.5 MW on the tritium resonance. As in the DD discharges at high ICRF power increased recycling is observed, resulting in high edge density. The high performance phase of this discharge was terminated by a sawtooth. The additional ICRF power does not increase the neutron yield and the fusion power reaches only 12.3 MW for a total input power of 25.1 MW (fig. 14).

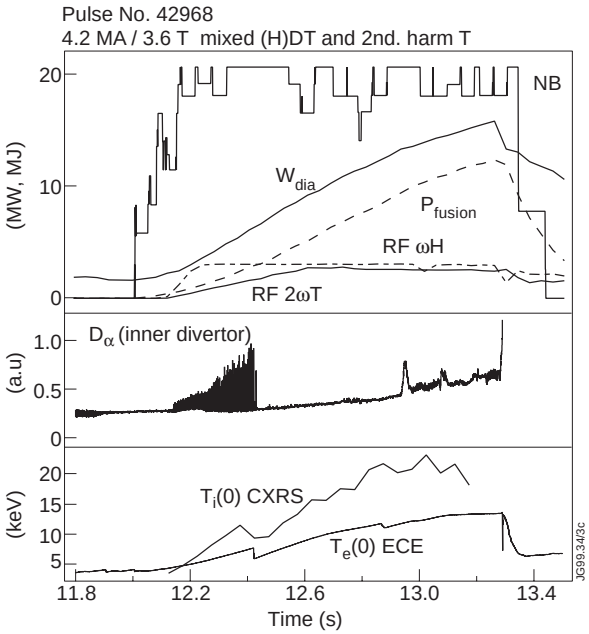

Fig.14: time evolution of plasma parameters for DT discharge No. 42968 at 4.2 MA / 3.6 T with mixed (H)DT and 2ωCT ICRF heating scenario. From top: additional heating power, DT fusion power, diamagnetic stored energy, edge D_α, core ion and electron temperatures.

4. NUMERICAL SIMULATIONS OF NB+ICRF ELM-FREE HOT-ION H-MODES

In parallel to the transport analysis with the TRANSP code, detailed simulations of DD and DT discharges have been carried out using the PION code, which includes a self-consistent treatment of RF damping and tail formation [9,31]. The code has recently been upgraded to deal with polychromatic scenarios. The NB ion distribution, deuterium or tritium, is taken into account by using the NB source rate profiles calculated by the CHEAP code [20] as function of time. In the following, the full simulation, NB + ICRF, is compared with a simulation of an artificial NB only case with the same plasma parameters of the actual discharge. This allows any direct ICRF contribution to the ion power balance and the neutron yield to be isolated from the effects due to increased electron temperature, which can be best assessed by comparison of actual NBI only and NBI+ICRF cases. It is worth noticing that, because the electron temperature and hence the critical energy E_{CRIT} are typically higher in the ICRF heated discharges, the PION code tends to overestimate the bulk ion heating in the simulation with NBI alone. As a consequence, the gain in bulk ion heating computed by taking the difference between the PION simulations with and without ICRF is somewhat underestimated.

For the cases considered here, the best match to the measured DD neutron rate is found for hydrogen concentration in the region of 2 - 3 %, which is within the error bars of what is measured in the experiments.

4.1 Deuterium plasmas with (H)D heating scenario

Both monochrome and polychrome scenarios have been simulated, to assess the effect of spreading the resonance on the power deposition and, more specifically, on the power split between species.

For a typical polychrome scenario, the code suggests (fig. 15) that initially most of the power is absorbed by the hydrogen minority. With increasing bulk ion pressure a larger power fraction, up to 40%, is absorbed by the deuteron population. Direct electron damping increases with electron pressure and is typically responsible for ≤ 10 % of the ICRF power absorption.

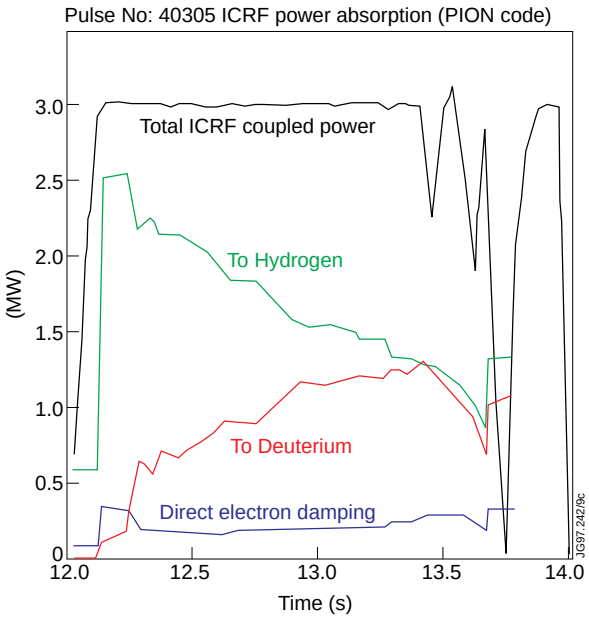

Fig.15: time evolution and of ICRF power absorption, computed by the PION code, for Pulse No. 40305

Most of the improvement in DD neutron yield with ICRF is due to particles with relatively low energy, with only 5 % of the neutron rate originating from energies above 150 keV (fig. 16).

The power absorbed by bulk ions or collisionally transferred from deuterium and, in a lesser extent, hydrogen tail is found to be roughly 50 % of the injected ICRF power, with 66% coming from deuterons. Since the power deposition is peaked on-axis, ICRF provides a substantial, ≅ 30 - 35 %, contribution to the ion power balance in the plasma core (fig. 17).

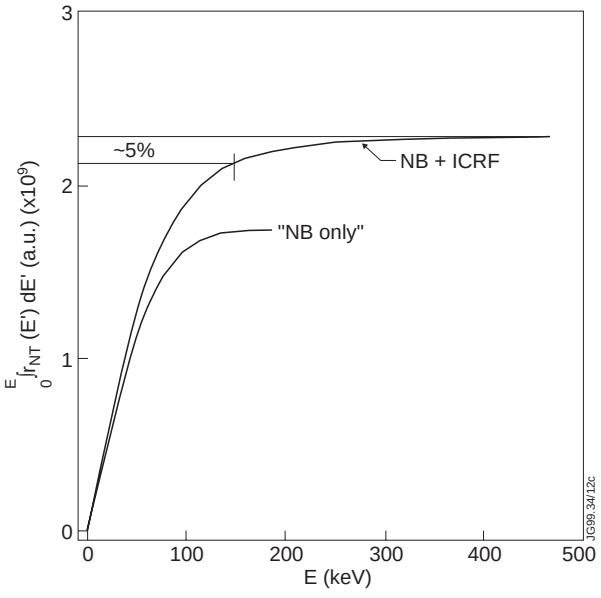

Fig.16: calculated DD neutron yield (PION code) as function of deuteron energy for Pulse No. 40305 close to the peak of DD neutron rate. The full NB+ICRF simulation is compared to a fictitious NB only case (see text).

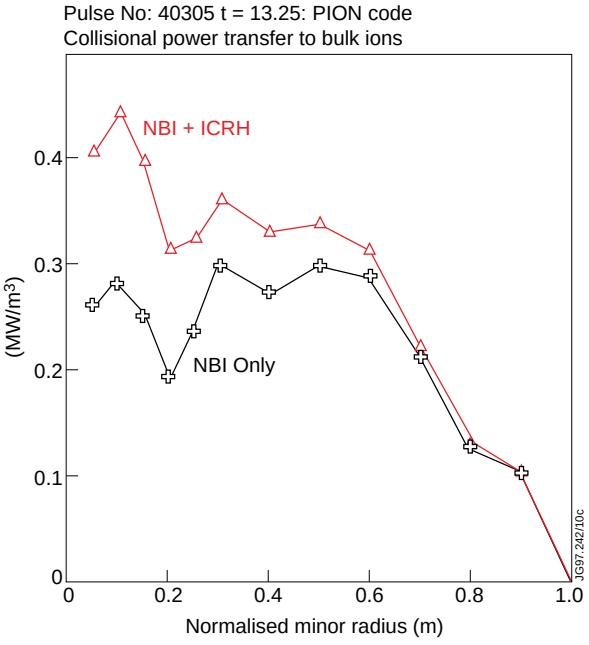

Fig.17: calculated collisional power transfer profile to bulk ions (PION code) for Pulse No. 40305 close to the peak of DD neutron rate. The full NB+ICRF simulation is compared to a fictitious NB only case (see text).

In comparison to the monochrome scenario, use of different frequencies to spread the ICRF power deposition yields results in a much reduced acceleration of the deuterium tail, a reduction of 20 % in fast ion energy and an increase of 5 to 10% in the power transferred collisionally to the bulk ions. A more detailed study of the differences between monochrome, polychrome, high and low RF power scenarios is presented elsewhere [32].

Simulations have also been carried out with the TRANSP code for NB+ICRF Hot-Ion H-modes. As already mentioned, it is found that in the combined heating case ion-electron equipartition is substantially reduced, up to half of the calculated value in the NBI only case. It is more difficult to quantify differences in the NB ion heating fraction due to the increased electron temperature, since ion heating already accounts for more than 80 % of the injected NBI power and the observed variations in the range of 10% are well within the uncertainties of the TRANSP modelling. On the other hand, it has to be noted that TRANSP does not have a self-consistent model for ICRF absorption and evolution of the deuterium distribution function ; hence, any enhancement of DD reactivity due to an RF driven deuterium tail is not taken into account. Nevertheless, TRANSP results for these cases show good agreement with the measured neutron yield and stored energy, again suggesting that contribution from a high energy deuteron tail is small.

4.2 Deuterium-tritium plasmas with (H)DT heating scenario

The overall physics picture of ICRF absorption and heating does not change substantially in going from (H)D to (H)DT. Nevertheless, in deuterium-tritium plasmas other resonances appear because of tritium and fusion born alpha particles, which could provide competing absorption mechanisms. More specifically, the third harmonic tritium resonance and the second harmonic alpha particle resonance coincide with the fundamental hydrogen and the second harmonic deuterium resonances. PION code calculations show, however, that such damping mechanisms are negligible in the JET DT plasmas analysed in this paper.

The simulation of one of the highest DT fusion performance discharges, #42974 at 4.2 MA / 3.6 T, shows excellent agreement with the measured DT neutron rate (fig. 18) and the diamagnetic stored energy, with the fast ion contribution due to RF accounting for 1 - 1.5 MJ. The calculations indicate that, at the peak of performance, the non-thermal DT fusion due to RF accelerated deuterons is of the order of 2 - 3 %.

As in the equivalent (H)D cases, ICRF power is initially absorbed almost exclusively by the hydrogen minority. By the end of the ELM-free phase, absorption at $2\omega_{CD}$ accounts for ~ 1.0 MW. Due to the increased electron pressure with respect to the DD cases, direct electron absorption via Electron Landau Damping (ELD) and Transit Time Magnetic Pumping (TTMP) is in the region of 0.5 MW or 15 % of the injected RF power. The partition of the power damping and collisional transfer to bulk ions and electrons is shown in fig. 19, highlighting the substantial contribution due to ICRF to the bulk ion input power.

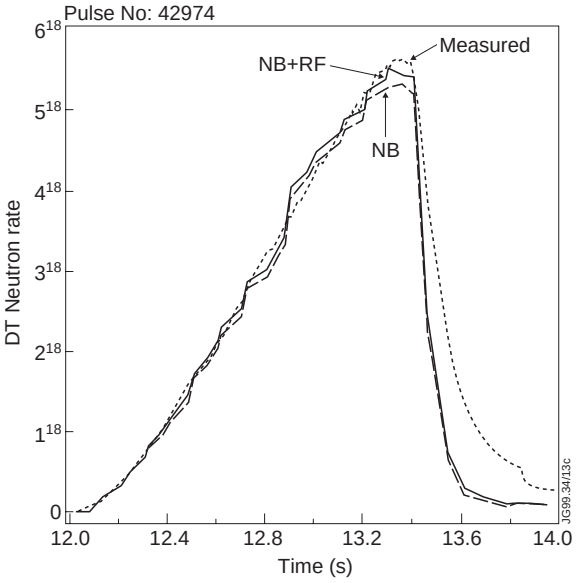

Fig.18: measured (solid) and computed (PION code) DT fusion rate for Pulse No. 42974. The full NB+ICRF simulation is compared to a fictitious NB only case (see text).

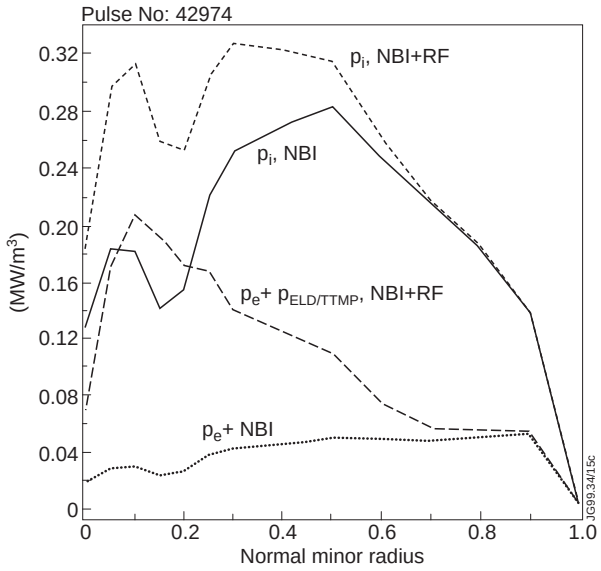

Fig.19: calculated collisional power transfer profile to bulk ions and electrons (PION code) for DT Pulse No. 42974 close to the peak of DD neutron rate. The full NB+ICRF simulation is compared to a fictitious NB only case (see text).

4.3 Deuterium-tritium plasmas with mixed (H)DT and $2\omega_{CT}$ heating scenario

The PION calculation for the mixed (H)DT + $2\omega_{CT}$ scenario indicates that most of the power tuned to the tritium resonance is absorbed directly by bulk electrons via ELD + TTMP. Only about 1 MW, out of 2.5 MW, is absorbed by tritons at the second harmonic resonance (fig. 20), with a negligible non-thermal contribution to the DT reactivity.

In total roughly 70 % of the ICRF power applied at $2\omega_{CT}$ is calculated to be transferred to bulk electrons, either through ELD+TTMP or collisionally from the triton distribution.

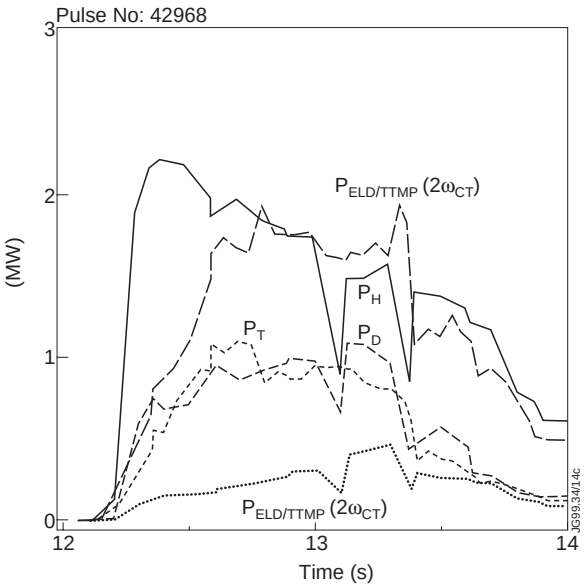

Fig.20: time evolution of ICRF power absorption (PION code) and power partition between different species for DT Pulse No. 42968, with mixed (H)DT and 2ωCT ICRF heating scenario.

5. SUMMARY AND CONCLUSIONS

Following promising results during the pre-PTE and the MKI divertor experiments, an extensive series of combined NB+ICRF Heating experiments in ELM-free Hot-Ion H-modes has been carried out during the deuterium phase of the JET MKIIa Divertor campaign. Up to

25 MW of total power were injected into single-null divertor plasmas with plasma current up to 4.2 MA and toroidal field up to 3.6 T. Most of the experiments were carried out using the (H)D heating scenario, either with single (monochrome) or multiple (polychrome) resonance positions; the (He^3)D scenario was also tested.

The addition of ICRF results in increased core electron and ion temperature and stored energy, up to a record of 14.5 MJ. The addition of ICRF enhances the DD fusion yield by up to 30%, extending the DD neutron yield for ELM-free Hot-Ion H-mode to 5.2×10^{16} neutrons/s. For moderate RF power, up to 3 - 4 MW, fusion performance scaling with input power and stored energy is equivalent to that with NBI alone. Discharges with modest RF polychrome power, show increased sawtooth stability in comparison with NBI only cases, and terminate with a combination of external kink modes and a giant ELM.

Simulations with the PION code indicate that up to 40% of the ICRF power is absorbed at the $2\omega_{CD}$ resonance by bulk and NB ions. Experimental confirmation of the presence of a Deuteron tail above the NB injection energy is provided by High Energy NPA data. Tail acceleration is minimised by polychrome operation, with a reduction of 20 % in fast ion energy and an increase of 5 to 10% in the power transferred collisionally to the bulk ions with respect to monochrome cases. ICRF power provides a 30 - 35 %, contribution to the ion power balance in the plasma core.

ICRF has been used in all but one of the 8 high power DT discharges in the ELM-free Hot-Ion regime. The addition of ICRF power at the $2\omega_{CT}$ resonance produced mainly electron heating and did not raise the fusion performance, but use of ICRF at the (H)DT scenario contributed to the achievement of a record DT fusion power of 16.1 MW and stored energy of 17 MJ.

The good agreement found between the experimental data and the simulations with the PION code indicates that we have a correct theoretical picture of the overall role that ICRF heating plays in the Hot-Ion ELM-free H-mode regime. The analysis of the (H)D heating scenarios has once more highlighted the complex interplay between absorption at the fundamental resonance and at higher harmonics with a pre-existent resonant fast ion population, in our case the injected NB deuterons. It has also demonstrated that ICRF heating can make a substantial contribution to the power input to the bulk ions in the plasma core.

In the MKIIa campaign progress has undeniably been made in the use and optimisation of ICRF heating in the Hot-Ion ELM-free regime, but several problems still remain open. In particular, in order to exploit the full power capability of the ICRF plant a method has to be found to apply higher power while avoiding increased recycling and without compromising sawtooth stability. One solution may lie in thorough high power conditioning of the ICRF antennas and careful tailoring of the time evolution of the applied ICRF power. The power could, for example, be limited at the beginning of the ELM-free phase and increased only later, once the bulk ion pressure has increased. A second route could be the use of the (He^3)D heating scheme. This

method, which could provide more bulk ion heating than the (H)D scenario, is severely power limited in the frequency range needed for operation at 3.4 T, but at higher values of toroidal field the frequency necessary, 37 - 42 MHz, would allow injection of substantially more ICRF power.

ACKNOWLEDGEMENTS

The authors gratefully acknowledge the support of the JET experimental Team and in particular of the Radio Frequency Division.

This paper is dedicated to the memory of Dr. D.F.H. Start, who died suddenly in August 1998.

REFERENCES

[1] T.T.C. Jones et al., Proc. of 38th Mtg. of APS Div. of Plasma Phys., Denver, USA 1996
[2] JET Team, Nucl. Fusion 32 (1992) 187
[3] M. Bures at al., Proc. of 19th EPS Conf. on Contr. Fusion and Plasma Phys., Innsbrück 1992
[4] G.Cottrell et al. Proc. of 23rd EPS Conf. on Contr. Fusion and Plasma Phys., Kiev 1996
[5] F.G. Rimini et al, in Radiofrequency Power in Plasmas (Proc. 11th Top. Conf. Palm Springs, 1995), AIP, New York (1996).
[6] A.C.Ekedahl et al., Nucl. Fusion 38 (1998) 1397
[7] P.R. Thomas et al., Phys. Rev. Lett. 25 (1998) 5548
[8] M. Keilhacker et al., Nucl. Fusion 39 (1999) 209
[9] L.-G. Eriksson et al., Nuclear Fusion 33 1037 (1993)
[10] L.-G. Eriksson et al., Nuclear Fusion 38 265 (1998)
[11] Cottrell et al, Proc. of 24th EPS Conf. on Contr. Fusion and Plasma Phys., Berchtesgaden 1997
[12] C.K. Phillips et al., Phys. Plasmas 2 (6) 1995
[13] T. H. Stix, Plasma Physics, 14, 367 (1972)
[14] The JET Team, presented by J Jacquinot, 18th EPS Conference on Plasma Physics and Controlled Fusion, Berlin, 1991
[15] Q.A. King, H.E.O. Brelén, JET-P(98)24 submitted for publication in Fusion Technology
[16] B. Balet et al, Nucl. Fusion 32 (1992) 1345
[17] H-MODE Database Working Group, Proc. of 20th EPS Conference on Plasma Physics and Controlled Fusion, Lisbon, 1993
[18] D.F.H. Start et al, in Radiofrequency Power in Plasmas (Proc. 11th Top. Conf. Palm Springs, 1995), AIP, New York (1996).
[19] M.F. Nave et al., Proc. of 24th EPS Conf. on Contr. Fusion and Plasma Phys., Berchtesgaden 1997

[20] M G von Hellermann et al. in Diagnostics for Experimental Thermonuclear Fusion Reactors , edited by P E Stott, G Gorini and E Sindoni, Plenum Press, New York and London, 1996, p. 281 ff.
[21] H.Y. Guo, submitted for publication in Nuclear Fusion
[22] M.F. Nave et al. , Nuclear Fusion 37 (1997) 809
[23] M.F. Nave et al., Proc. of 25th EPS Conf. on Contr. Fusion and Plasma Phys., Prague 1998
[24] G.T.A Huysmans, T.C. Hender, B. Alper, Nuclear Fusion 38 (1998) 179
[25] A. Fasoli et al, Plasma Phys. And Controlled Fusion, vol. 39 suppl. 12B, page B287 December 1997
[26] D. Borba et al., Proc. of 5th IAEA Technical Committee Meeting on Alpha Particles in Fusion Research, 8-11 Sept. 1997, UK
[27] S. Sharapov et al., Proc. of 25th EPS Conf. on Contr. Fusion and Plasma Phys., Prague